

Recent modifications to the ImageStream® technology improving its applicability to the study of NF-κB activation in a clinical research setting



George TC¹, Venkatachalam V¹, Zimmerman C¹, Perry D¹, Ortny WE¹, Collins C² and Minderman H².
¹Amnis Corp., 2505 3rd Ave, Ste 210, Seattle, WA. ²Roswell Park Cancer Institute, Buffalo, NY.

Abstract

During the first year of funding the emphasis of the work has been to increase data collection speed, sample throughput, focus quality of collected images, flexibility of excitation sources and optimizing analysis algorithms. **Data collection speed/sample throughput:** In the original architecture of the ImageStream, 5000 events of a 1x10⁶ cell standard sample took 8 min. to acquire and the in-between sample wash cycle took 8 min., giving an overall sample throughput of 4 samples/hr. Hardware and fluidic script changes now collect 5000 events of a 1x10⁶ cell sample and wash in 5 minutes, giving a throughput of 12 samples/hr. **Focus quality:** The image focus quality has been improved by installation of an extended depth of field (EDF) optical element, which extends the depth of focus from 2 μm to 16 μm. The EDF principle is based on the ability to develop an optical Point Spread Function (PSF) that is invariant to focus over a range equivalent to the diameter of a large cell (~15 μm). If the PSF remains invariant, it can be mathematically, thereby producing an image of the entire cell in focus. The EDF option uses a Wavefront Coded[®] element developed by CDM Optics (Boulder, CO) which substantially changes the size and nature of the PSF. Since initial beta launch, changes to hardware, calibration routines, and deconvolution algorithms have substantially improved the EDF element's PSF invariance to focus. When combined with the newly developed and greatly improved deconvolution techniques the resulting imagery has noticeably fewer artifacts, maintains a natural appearance and leads to an overall improved image quality. **Excitation sources:** The basic commercial release of the ImageStream has a single 488nm excitation source. Corrections for the blue-channel image size difference (associated with a 405nm laser excitation) and the red laser scatter leakage into channel 5 of the ImageStream (associated with a 658nm red laser) have now been solved. Combined, the above modifications improved the overall effectiveness and applicability of the ImageStream, not only with regards to assessment of NF-κB translocation but also in all applications of the system. **Analysis algorithms:** The current analysis algorithm uses a 'similarity score' which is a log transformed Pearson's correlation coefficient of the pixel values of the DRAQ5 (nuclear) and NF-κB images. If NF-κB is localized to the nucleus, the two images are similar and a large positive value is generated. If NF-κB is cytoplasmic, the two images are anti-similar and a large negative value is generated. Changes in the distributions can be reported as a % shift into a rigorously set translocated gate; this requires a decision on how much nuclear NFκB is considered base-line, or can be reported as an Rd metric which is a measure for the shift of two distributions (taking into consideration their respective median and standard deviations). Alternatively, the nuclear translocation of NF-κB can be measured as the relative nuclear concentration compared to the whole cell concentration. The effects of data acquisition (with or without EDF), nuclear segmentation algorithms (how the nuclear area is defined) and accuracy and reproducibility of these analysis approaches are currently studied. This work funded through grant R21 CA126667-01

Introduction

The functions of many key proteins controlling cell growth and survival such as tumor suppressors and transcription factors are, amongst other factors, also dependent on cellular localization. Homeostatic as well as reactive conditions require proper signal transduction between the cytoplasm and nucleoplasm achieved by a regulated shuttling of proteins across the nuclear envelope through nuclear pore complexes. In cancer, aberrant signal transduction is commonly observed and novel therapeutic agents targeting these signaling cascades are currently evaluated in clinical trials or have already secured a position in the therapeutic arsenal. Aberrant signal transduction is often associated with increased intracellular distribution of specific signaling intermediates, thus their sub-cellular localization could potentially be used as a parameter of therapy response.

Nuclear-cytoplasmic shuttling events have typically been studied by molecular techniques or by (confocal) microscopy which have the disadvantage of lack of specificity for target cell populations and lack of high throughput screening capability. Amnis Corporation, Seattle, WA, has developed the ImageStream multiplexed imaging flow cytometer. This platform produces high resolution brightfield, laser side scatter, and fluorescence images of cells prepared in suspension at rates exceeding 100 cells per second. The IDEAS™ analysis software quantifies hundreds of morphometric and photometric parameters for each cell based on its imagery, including parameters that measure sub-cellular location of probes. The aim of this proposal is to evaluate the potential of multiplexed imaging flow cytometry to evaluate target cell-specific, therapy-induced, changes in nuclear-cytoplasmic distributions as response parameters in clinical samples from patients with acute myeloid leukemia (AML) and multiple myeloma (MM) undergoing therapy with the macrolide rapamycin (sirolimus) or the proteasome inhibitor bortezomib (velcade), respectively. Both agents are known to affect the function (and cellular localization) of nuclear factor-κB (NF-κB) which is aberrantly activated in AML and MM. The R21 phase of this proposal will evaluate the technique's ability to quantify nuclear-cytoplasmic distributions of NF-κB. During this phase, system hardware, software and sample preparation conditions will be optimized using NF-κB as a model system. Applicability of detecting other proteins associated with NF-κB signal transduction and rapamycin and bortezomib action, their localization with other cell organelles and co-localization will also be assessed. The success of defining other applications in addition to NF-κB will be used to generate additional hypotheses for testing in the R23 phase of this proposal. The R23 phase will apply this technique in the analysis of patient samples and will test the hypothesis that cellular distribution of NF-κB can be used as a determinant of response in AML patients treated with rapamycin or MM patients treated with bortezomib, as well as additional hypotheses generated in the R21 phase.

Materials and Methods

Focus Pan:

2.5 micron diameter fluorescent beads (Invitrogen) were run on the ImageStream in standard or EDF mode. The beads are sufficiently small relative to the pixel size and diffraction limited spot size of the ImageStream optics to be treated as point sources. 2000 bead images were collected (with autofocus turned off) at 1 micron increments across a 16 micron z-axis range.

NF-κB localization in THP-1 cells:

THP-1 cells were treated with 100 ng/mL LPS or media alone for 45 minutes at 37 C. The cells were then fixed with 4% formaldehyde/PBS for 10 min at RT, then stained in perm buffer (0.1% TritonX100/2%FBS/PBS) with FITC anti-p65 (Santa Cruz sc-372, rabbit polyclonal) for 20 min at RT, followed by staining with FITC F(ab)₂ donkey anti-rabbit (Jackson ImmunoResearch 711-096-152) for 10 min at RT. The cells were then run in 5 μm DRAQ5 on the ImageStream in standard and EDF imaging mode.

NF-κB localization in ML1 cells:

ML1 cells were treated with 10 ng/mL TNF-α or media alone 30 minutes at 37 C. The cells were then fixed with 4% formaldehyde/PBS for 10 min at RT, then stained in perm buffer (0.1% TritonX100/2%FBS/PBS) with FITC anti-p65 (Santa Cruz sc-372) for 20 min at RT, then run in 5 μm DRAQ5 on the ImageStream in standard and EDF imaging mode.

Statistics - Fisher's discriminant ratio (Rd):

Overlapping distributions are common to the inherent heterogeneity of cell biology. We use a statistical method to determine differences between experimental and control samples. We use the Fisher's Discriminatory Ratio (Rd) to represent the degree to which measured distributions can be distinguished from one another, and is given by the following formula:

$$Rd = \frac{\text{MedianExp} - \text{MedianNeg}}{\text{SDExp} + \text{SDNeg}}$$

Any experimental sample can be evaluated in relation to the Rd between the biological positive and negative control. To the extent possible, we try to maximize the Rd between the controls by optimizing experimental conditions, sample prep, and analytical approach.

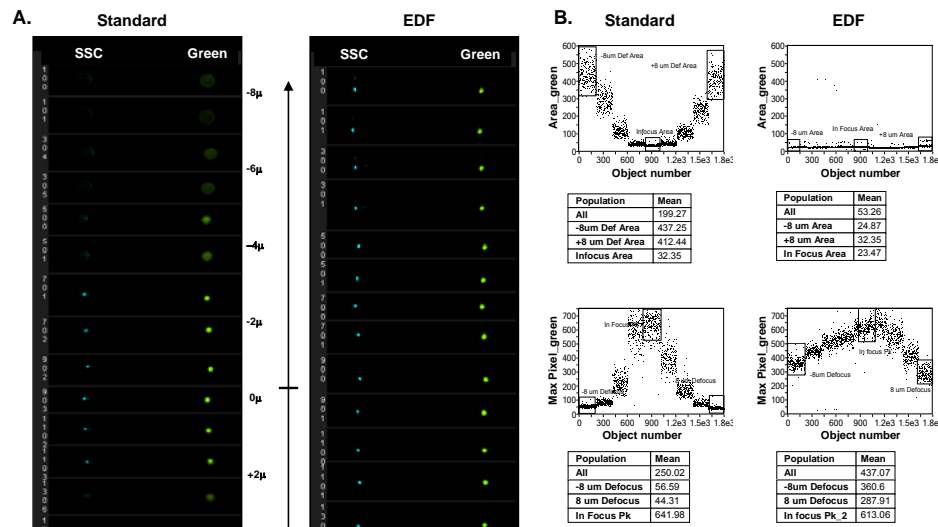


Figure 1: EDF imaging extends the ImageStream depth of field to 16 μm

ImageStream standard (left panel) and extended depth of field (right panel) 2.5 micron green fluorescent bead imagery collected over a 16 micron focus pan. Left and right panels show both laser side scatter (blue) and fluorescence (green) imagery (A). Standard image collection exhibits significant blur while extended depth of field imagery maintains size and concentration of intensity throughout the entire 16 micron focus pan. To quantify the effect of focal position on quantitative focus, we measured the area and the max pixel of the green image across the focus pan. Bead images in best focus have their intensity concentrated in small areas, and thus have high max pixel and low area values. Comparison plots of Max Pixel and Area of the green bead image for standard and extended depth of field imaging modes of 2.5 micron beads collected over a 16 micron focus range are shown in (B). Dot plots show feature values (Area or Max Pixel of the green image) plotted against focal position (object number). Extended depth of field image collection demonstrates 7 - 14 times less variation over the tested focal range.

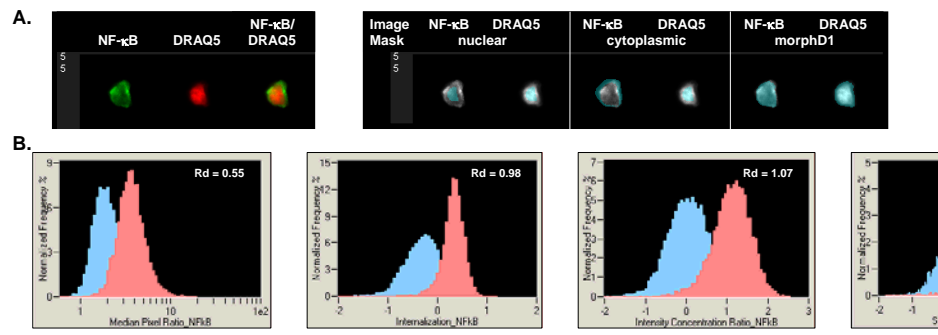


Figure 2: Effect of imaging mode and core diameter on nuclear translocation quantification

THP-1 cells were incubated in media (Untreated) or 100 ng/mL LPS for 45 minutes, then fixed, permeabilized and stained with FITC anti-NF-κB (green) and DRAQ5 (red). Untreated (230,000 cells per test suspended at 4.7E+06 cells/mL) and LPS sample pairs were run on the ImageStream using various configurations to determine the impact of these instrument run settings on cellular throughput, image quality and statistical discrimination of the sample pair using the Similarity feature as a measure of translocation. The instrument configurations compared were: 10 micron vs 15 micron core diameter; Standard imaging vs EDF imaging; 1X binning (standard) vs 2X binning. Here we compare the image quality of the sample pairs run using the standard configuration (10 micron core, standard imaging mode, 1X binning) to left to the pairs run using maximum throughput mode (15 micron core, EDF imaging, 2X binning; the throughput in this mode is 6X standard) (A). Similarity, NF-κB/DRAQ5 overlays for single cells (no focus gate) of both conditions are plotted in (B) with the Rd indicated in the upper right corner. These data indicate that the increased depth of field afforded by the EDF element enables higher resolution imaging even when the core is widened and the vertical pixel is binned by a factor of 2. The full quantitative comparisons amongst the imaging modes are displayed in Table 1.

Table 3.

Channel 1 470-500nm	Channel 2 400-470nm	Channel 3 500-560nm	Channel 4 560-595nm	Channel 5 595-660nm	Channel 6 660-735nm
SSC	Brightfield	Brightfield	Brightfield	Brightfield	Brightfield
	DAPI*	Fluorescein	PE	7-AAD	PE-Cy5.5
	Pacific Blue*	AF488	Cy-3	AF610/PE	PE-Cy5.5
	Cascade Blue*	GFP	DSRed	AF680/PE	
	Marina Blue*	Syto Green	PE-TexasRed	AF647/PE	
	AF430*	Spectrum Green	ECD	Draq-5	
	AF405*	YFP		3D-705	
	Sybr Green			AF647**	
	Pacific Orange*			AF680**	
				Cy5**	

Table 4.

Channel 1 470-500nm	Channel 2 400-470nm	Channel 3 500-560nm	Channel 4 560-633nm	Channel 5 633-660nm	Channel 6 660-735nm
SSC	Brightfield	Brightfield	Brightfield	Brightfield	Brightfield
	DAPI*	Fluorescein	PE		PE-Cy5.5
	Pacific Blue*	AF488	PI		PE-Cy5.5
	Cascade Blue*	GFP	Cy3**		AF680/PE
	Marina Blue*	Syto Green	DSRed**		AF647/PE
	AF430*	Spectrum Green	Spectrum Orange**		PerCP
	AF405*	YFP	mCherry**		PerCP-Cy5.5
	Sybr Green				Draq-5
	Pacific Orange*		AF555**		QD-705
			AF680**		7AAD**

Figure 4: Fluorochrome chart for three-laser ImageStream systems

Amnis commercially released 2 additional lasers (90 mW 658 nm and 350 mW 405 nm) as upgrade options to the base ImageStream (200 mW 488 nm) system in order to increase the number of common fluorochromes compatible with the system (Table 3). Correction optics for blue-channel image size difference and filters to prevent red scatter from reaching the camera were added as part of the upgrade. A custom 405 nm/561 nm (100 mW) laser upgrade was done at RPCL. An optimized 561 nm notch filter (561/16nm) prevents 561 nm scatter from reaching the camera. The common fluorochromes compatible with the 405/488/561 system are shown in Table 4.

Table 2.

Feature	Untreated		TNF-α		Rd
	Med	SD	Med	SD	
Median Pixel Ratio	1.99	1.43	3.61	1.54	0.55
Internalization	-0.28	0.37	0.33	0.25	0.98
Intensity Concentration Ratio	0.06	0.52	1.13	0.49	1.07
Similarity	0.39	0.51	1.64	0.48	1.26

Figure 3: Statistical determination of the best image-based feature for measuring nuclear translocation

Quantitative image analysis affords objective discrimination of cells based on their imagery, and involves application of mathematical algorithms to defined regions of the cellular image. The IDEAS® image analysis software program has hundreds of features (algorithms) and 13 different masking operations (region-finders), enabling highly sophisticated image-based analysis for tens of thousands of cells per sample. To determine which feature/mask combination provides the best method for measuring nuclear translocation, we use Rd analysis between a positive and negative biological control. In this experiment, ML1 cells were incubated in media alone (Untreated, negative biologic control) or 10 ng/mL TNF-α for 30 min, then fixed, permeabilized and stained with FITC anti-NF-κB (green) and DRAQ5 (red). 10,000 events were collected on the ImageStream in EDF mode, and nuclear translocation was quantified using four methods (Masks shown in A, overlay histograms in B):

Median Pixel Ratio = Median NF-κB Pixel within the nuclear mask (A) / Median NF-κB Pixel within the cytoplasmic mask.

Internalization = NF-κB bright intensity within the nuclear mask ratio'd to the NF-κB bright intensity outside the nuclear mask. Given by the following formula:

$$\text{Internalization} = \log \left(\frac{a - \frac{p_1}{p_2}}{1 - \frac{p_1}{p_2}} \right), \text{ where } a = \frac{m_1}{m_1 + m_2}$$

where i = nuclear mask; b = area outside the input mask; m = mean intensity of the upper quartile pixels in the given mask; p = max pixel in the given mask.

Intensity Concentration Ratio = NF-κB bright intensity within the nuclear mask ratio'd to the NF-κB bright intensity within the cytoplasm mask (formula same as internalization, except mask b is the user-defined cytoplasm mask).

Similarity = pixel-by-pixel correlation of the NF-κB and DRAQ5 image pair within the nuclear morphology mask, dilated one pixel (morph).

Table 2 shows the median, standard deviation, and Rd for the four features between untreated and TNF-α-treated samples, with the Rd plotted in C. These data indicate that for these cells, Similarity provides the greatest discrimination between the standard.

Table 1.

Treatment	Core Diameter (μm)	Image Mode	Bin mode	Focus cells/sec	Fold Increase in Throughput	Similarity NFκB/DRAQ5		
						Median	Std Dev	Rd
Untreated	10	STD	1	6.5	-0.84	0.78		
LPS	10	STD	1	6.3	2.84	0.85	2.26	
Untreated	10	EDF	1	10.0	1.2	-0.8	0.51	
LPS	10	EDF	1	9.1	1.4	-0.86	0.63	2.39
Untreated	10	STD	2	14.9	1.8	-0.86	0.75	
LPS	10	STD	2	12.0	1.9	2.97	0.83	2.43
Untreated	10	EDF	2	20.2	2.4	-0.76	0.5	
LPS	10	EDF	2	17.5	2.1	2.93	0.66	2.42
Untreated	15	STD	1	11.4	1.7	-0.78	0.84	
LPS	15	STD	1	11.4	1.8	2.87	0.81	2.21
Untreated	15	EDF	1	24.0	2.8	-0.78	0.51	
LPS	15	EDF	1	20.7	3.3	1.86	0.64	2.3
Untreated	15	STD	2	31.4	3.7	-0.72	0.87	
LPS	15	STD	2	22.5	3.6	3.06	0.85	2.2
Untreated	15	EDF	2	50.5	5.9	-0.82	0.54	
LPS	15	EDF	2	41.0	6.5	2.02	0.68	2.33

1X vertical bin, corresponding to a 0.5 micron x 0.5 micron resolution per pixel
 2X vertical bin, corresponding to a 1.0 micron x 0.5 micron resolution per pixel
 Untreated (230,000 cells per test suspended at 4.7E+06 cells/mL)
 LPS = 100 ng/mL for 45 minutes (200,000 cells per test suspended at 4.1E+06 cells/mL)
 Focused cells selected as those events with high Gradient RMS_DRAQ5 values

Table 1: Effect of imaging mode and core diameter on ImageStream throughput and nuclear translocation quantification

Operating in the standard resolution setting, we normally run the instrument at 90% of the maximum camera line rate. To maximize acquisition rate given the line rate limit inherent to the camera, we combined vertical pixel binning (to enable twice the flow speed at the maximum line rate) with widening the core diameter from the standard 10 microns to 15 microns. Because sample throughput is related to the square of the core diameter, we expect that widening the core in this manner would further increase throughput a little over two-fold. Because widening the core diameter naturally increases the percentage of cells that flow out of the optimal plane of focus, we used the extended depth of field (EDF) optical element, which extends the ImageStream depth of focus from 2 microns to 16 microns. The EDF element is expected to bring all cells running in a 15 micron core in focus. We evaluated the impact of binning, core diameter, and imaging mode on throughput, image quality, and statistical analysis of LPS-induced nuclear translocation in THP-1 cells (Table 1). We observed a substantial increase in throughput when imaging a 15 micron core in 2X bin mode with the EDF element compared to results obtained when operating the instrument conventionally with 10 micron core, without binning or EDF (6 fold for LPS, 6.5 fold for untreated). Of note, 100% of the cells in all EDF samples, including those collected with a 15 micron core, were in focus. Furthermore, the statistical separation (Rd) of the Similarity score distributions between the untreated and LPS treated samples were essentially unchanged when imaging in the highest throughput mode.